



OPEN ACCESS

EDITED BY

Mohamed Ashour,
National Institute of Oceanography and
Fisheries (NIOF), Egypt

REVIEWED BY

Gamal Ammar,
City of Scientific Research and Technological
Applications, Egypt
Ahmed E. Alprol,
National Institute of Oceanography and
Fisheries (NIOF), Egypt
Ghada Farouk El-Said,
National Institute of Oceanography and
Fisheries (NIOF), Egypt

*CORRESPONDENCE

Meseret Dawit Teweldebrihan,
✉ mesedawit@gmail.com

RECEIVED 30 January 2024

ACCEPTED 26 March 2024

PUBLISHED 11 April 2024

CITATION

Teweldebrihan MD, Gnaro MA and Dinka MO
(2024), The application of magnetite biochar
composite derived from parthenium
hysterophorus for the adsorption of methylene
blue from aqueous solution.
Front. Environ. Sci. 12:1375437.
doi: 10.3389/fenvs.2024.1375437

COPYRIGHT

© 2024 Teweldebrihan, Gnaro and Dinka. This is
an open-access article distributed under the
terms of the [Creative Commons Attribution
License \(CC BY\)](https://creativecommons.org/licenses/by/4.0/). The use, distribution or
reproduction in other forums is permitted,
provided the original author(s) and the
copyright owner(s) are credited and that the
original publication in this journal is cited, in
accordance with accepted academic practice.
No use, distribution or reproduction is
permitted which does not comply with these
terms.

The application of magnetite biochar composite derived from parthenium hysterophorus for the adsorption of methylene blue from aqueous solution

Meseret Dawit Teweldebrihan^{1*}, Mikiyas Abewaa Gnaro² and
Megersa Olumana Dinka¹

¹Department of Civil Engineering Sciences, Faculty of Engineering and the Built Environment, University of Johannesburg APK Campus, Johannesburg, South Africa, ²Department of Chemical Engineering, College of Engineering and Technology, Wachemo University, Hossana, Ethiopia

The removal of toxic and harmful dyes like methylene blue (MB) from textile wastewater is necessary to reduce environmental pollution. Therefore, this study is aimed at removing MB from an aqueous solution using magnetite-doped biochar of parthenium hysterophorus. Biochar was prepared through pyrolysis techniques at 500 °C for 2 h whereas the magnetite and composite material were developed using coprecipitation methods. Herein, NaNO₃ and FeSO₄ · 7H₂O were utilized as precursor materials and NaOH as a precipitating agent for preparation of magnetite. Furthermore, pH point of zero charge (pHpzc), Scanning Electron microscope (SEM), Fourier Transform Infrared Spectroscopy (FTIR), and X-ray Diffraction (XRD) are characterization techniques used to evaluate the nature of the composite material. On the other hand, a full factorial design involving four factors at two levels (2⁴) such as pH (3 and 9), contact time (10 and 40 min), initial dye concentration (100 and 150 mg/L) and adsorbent dosage of 0.01 and 0.04 g/100 mL was used to design and optimize the batch adsorption of MB from an aqueous solution. As a result, a maximum removal efficiency of 99.99% was attained at optimum operating conditions of pH 9, contact time 40 min, initial MB concentration 100 mg/L and adsorbent dosage of 0.04 g/100 mL. Langmuir, Freundlich and Temkin isotherm models were used to investigate the adsorption isotherm in which Freundlich isotherm with a maximum R² of 0.98 was found to describe the adsorption process inferring multilayer and heterogeneous surface interaction. Additionally, the thermodynamics study depicts that the nature of the adsorption is spontaneous, endothermic and feasible. On the other hand, the chemisorption nature is revealed by the pseudo second kinetics model with a maximum R² of 0.99. Finally, the remarkable reusability ranging from 99.98% to 97.6% for five consecutive cycles proved that the magnetic biochar derived from parthenium hysterophorus can be used as an effective adsorbent for the decolorization of MB saturated effluent at an industrial scale.

KEYWORDS

methylene blue, parthenium hysterophorus, magnet biochar, wastewater treatment, textile wastewater

1 Introduction

Water pollution is the contamination of natural water bodies by chemical, physical, radioactive or pathogenic microbial substances. It can result in large scale illness and deaths, with approximately 50 million deaths per year worldwide, mostly in Africa and Asia (Gautam, 2019). Furthermore, water pollution can impair the beneficial use of a water body, depending on its type, location, and the uses it supports. Anthropogenic sources of pollution, arising from human activities, are the main cause of water pollution (Schweitzer and Noblet, 2018). Normally, water pollution can arise from many sources, including mining, manufacturing, farming, power production, and urban and suburban sprawl (Babuji et al., 2023). These activities introduce toxic chemicals and pollutants into water bodies, impacting both surface and groundwater systems (Tang et al., 2022). Wastewater is generated globally from various sources including domestic, industrial, and agricultural sectors. Domestic wastewater consists of water from household activities, while industrial wastewater comes from sectors such as food, chemical, and power industries. Agricultural wastewater is generated from farming activities (Jones et al., 2023). These wastewaters contain organic and inorganic pollutants that can have detrimental effects on the environment (Zahoor and Mushtaq, 2023). Particularly, industrial wastewaters are the undesired aqueous discards generated through various industrial activities (Meena et al., 2022). They generally contain high concentrations of toxic or non-biodegradable pollutants such as Chemical Oxygen Demand (COD), Biochemical Oxygen Demand (BOD), Total Solids (TS), Total Dissolved Solids (TDS), Total Suspended Solids (TSS), inorganic ions, and other pollutants (Kishor et al., 2021). Industrial wastewater is high in organic matters, nutrients, and microorganisms, which exceed the allowable limits (Ajiboye et al., 2021). Additionally, it contains toxic pollutants such as dyes, heavy metals, surfactants, personal care products, pesticides, and pharmaceuticals, which drastically change water quality. The pollutants present in industrial wastewaters vary depending on the industry (Ahmed et al., 2021; Ajiboye et al., 2021; Pereira et al., 2022). For example, textile wastewater effluent contains hazardous substances such as dyes, pigments, solids and heavy metals (Khan et al., 2023).

Textile wastewater is characterized by intense color, high pH, high temperature, and high levels of chemical oxygen demand (COD) and total suspended solids (TSS) (Khan et al., 2023). It also contains various pollutants such as dyes, dissolved solids, suspended solids, toxic metals, pesticides, surfactants, volatile organic compounds, and heavy metals (Azanaw et al., 2022). These pollutants can have detrimental effects on the environment and living organisms, including reducing seed germination and biomass production of plants (Dhruv Patel and Bhatt, 2022). Toxic dyes such as methylene blue (MB) in particular have detrimental effects on the human health and the environmental ecology. MB is a cationic dye commonly used in industries for dyeing fabrics, papers, and leathers. It is environmentally persistent, toxic, carcinogenic, and mutagenic, posing a threat to human health and the environment (Oladoye et al., 2022). MB is released into groundwater and surface water through wastewater, leading to contamination. Moreover, MB has also been studied for its potential risks and adverse effects on human health. It can cause

symptoms such as hemolysis, methemoglobinemia, nausea, chest pain, and hypertension (Bužga et al., 2022). However, MB has also been utilized for its beneficial properties. It has been used as an antimalarial agent, an antioxidant, and an antifungal agent in the treatment of malaria, Alzheimer's disease, and candidiasis, respectively (Posso et al., 2022). Overall, MB has both negative environmental and human health impacts, but it also has potential applications in various fields. Therefore, it is essential to treat MB saturated wastewater before its discharge into water bodies to prevent contamination and harm to aquatic life (Santoso et al., 2020).

Various removal strategies have been explored, with adsorption technology being the most promising (Rajendran et al., 2022). Adsorption studies have been conducted for the removal of methylene blue dye using various adsorbents. Al-Qaim et al. investigated the use of fig leaf-activated carbon (FLAC-3) for the adsorption of methylene blue dye, achieving an adsorption capacity of 24.75 mg/g and following the Langmuir isotherm model (Al-Asadi et al., 2023). Another study by Nabi and Bari focused on the adsorption of methylene blue on activated carbon derived from bituminous coal, with the Langmuir isotherm being considered the most appropriate model (Alouiz et al., 2023). Mustapha et al. evaluated the adsorptive capacity of elephant grass for the removal of methylene blue dye, finding that the adsorption data best fit the Langmuir isotherm model (Mustapha et al., 2023). These studies demonstrate the effectiveness of different adsorbents in removing methylene blue dye through adsorption processes.

Biochar and biochar composites have shown potential for methylene blue adsorption from wastewater. Biochar from *Fructus Aurantii Immaturus* residues has high adsorption capacity due to its abundant functional groups and high porosity (Mustapha et al., 2023). Biochar composites made from wheat straw and biomass fly ash show enhanced MB adsorption capacity and high performance over various pH ranges (Li et al., 2023). Cigler and Hessian synthesized hematite-biochar composites using microwave-assisted pyrolysis, iron oxide-hydrochar composites, and mineral-biochar composites, demonstrating improved adsorption capacities for MB due to oxygen-containing functional groups and higher cation exchange capacity (Astuti et al., 2023). Pristine biochar has limitations in terms of its surface area, porosity, and surface functional groups, which can affect its physicochemical and functional properties (Chhimwal et al., 2022). Additionally, the synthesis of biochar for extended applications may compromise specific reaction conditions, and the separations and recyclability of biochar in smaller grinded powder form can be challenging (Mishra et al., 2023). Furthermore, the increasing types and quantities of potentially toxic elements in the environment have exceeded the scavenging capacity of pristine biochar (Batool et al., 2022; Mishra et al., 2023). However, modifications of biochar, such as through impregnation with various chemical entities, can enhance its sorption potential and make it more effective in removing potentially toxic elements (Ahuja et al., 2022). Overall, the limitations of pristine biochar can be addressed through modification techniques to enhance its properties and broaden its applications (Lebrun et al., 2018).

Engineered biochar (EBC) offers several advantages over pristine biochar (PBC). EBCs have improved physicochemical properties, such as increased specific surface area and pore

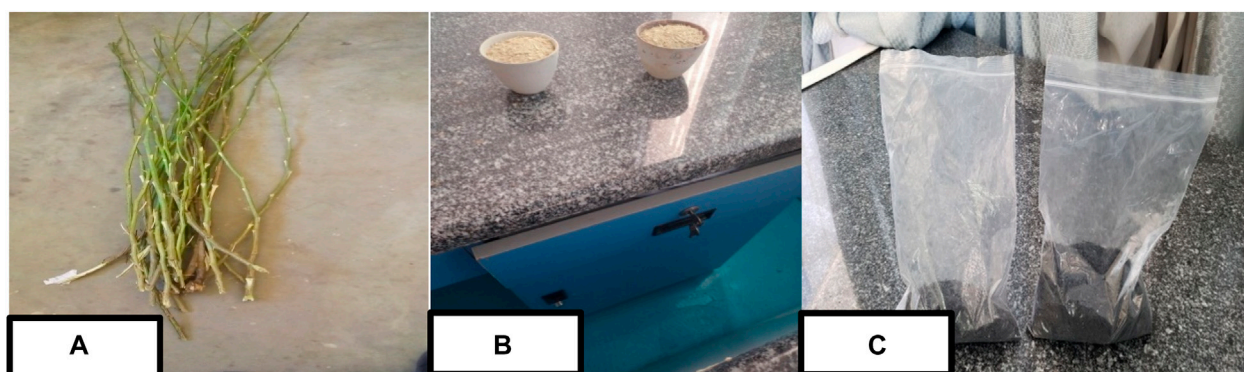


FIGURE 1
Essential parthenium hysterophorus biochar preparation stages; a raw parthenium hysterophorus stem (A), dried powdered sample (B) and parthenium hysterophorus biochar (C).

characteristics, which enhance their adsorption capacity for pollutants (Kazemi Shariat Panahi et al., 2020). The modification of biochar through impregnation with metals or metal oxides, such as zinc (Zn) and iron (Fe) oxides, significantly enhances its adsorption performance for contaminants like selenite (Se (IV)) (Islam et al., 2021). EBCs also show reduced content of toxic substances, such as polycyclic aromatic hydrocarbons (PAHs), compared to PBCs (Anae et al., 2021). Additionally, EBCs have been found to be efficient in removing various pollutants, including antibiotics, dyes, metals, and nutrients, from contaminated water (Murtaza et al., 2022). These advantages make EBCs a promising material for wastewater treatment, soil amendment, and environmental remediation.

Parthenium hysterophorus is an invasive weed species that poses a significant threat to cereal crops and livestock (Malik et al., 2023). Its growth and fecundity are influenced by soil pH, with acidic soil promoting accelerated growth and flowering (Ghazali et al., 2023). Hence, the detrimental impact of parthenium hysterophorus on the environmental ecology necessitates effective management strategies. One way of effectively managing parthenium hysterophorus is through utilizing it for adsorbent preparation (Ejaz et al., 2022). Parthenium hysterophorus based activated carbon has been studied for adsorption of pollutants in various industries, including tannery wastewater and textile wastewater (Bedada et al., 2020; Fito et al., 2020). Biochar derived from parthenium hysterophorus has been shown to improve soil health, crop performance and agronomic performance (Muche et al., 2022). On the other hand, magnetic biochar is a promising adsorbent for the treatment of organic and inorganic pollutants in water (Wen et al., 2021). It has high adsorption capacity and adsorption rate, making it effective for the removal of toxic contaminants from wastewater. Normally, magnetite doping can improve the catalytic capability of the biochar and enhance its adsorption and degradation of pollutants (Feng et al., 2021). Therefore, this study intends to remove MB from an aqueous solution using magnetite - biochar composites derived from parthenium hysterophorus. So far, the application of magnetic biochar composite for MB remediation is lacking which highlights the existence of the research gap.

2 Materials and methods

2.1 Adsorbent preparation

Biochar was prepared from parthenium hysterophorus biomass following the procedures described in (Sutar and Jadhav, 2024). Precisely, the precursor material was collected from Addis Ababa, Ethiopia. The collected parthenium hysterophorus sample was thoroughly washed and rinsed with tap and distilled water respectively. Then, the sample was allowed to dry in sunlight for 5 days and then placed in the oven at 105 °C overnight. Thereafter, the moisture freed sample was size reduced and pyrolyzed at a temperature of 500 °C for 2 h following the procedures described in Fito et al. as shown in Figure 1, where A is a raw parthenium hysterophorus stem, B is dried powdered sample and C is parthenium hysterophorus biochar (Fito et al., 2023b).

Additionally, magnetite was synthesized using the coprecipitation method using NaNO_3 and $\text{FeSO}_4 \cdot 7\text{H}_2\text{O}$. This method offers a simple and facile approach for the synthesis of Fe_3O_4 particles with superparamagnetic characteristics and aggregated morphology in high purity. Likewise, coprecipitation method was used for the preparation of magnetite biochar composite derived from parthenium hysterophorus utilizing NaOH as a precipitating agent. The synthesis process involves loading iron oxide particles onto the surface of the biochar through a simple coprecipitation method following the procedures described elsewhere (Frolova, 2019). Figure 2A, B are magnetite and magnetite biochar composite derived from parthenium hysterophorus respectively.

2.2 Adsorbent characterization

The mass addition method was used to determine the pH point of zero charge (pHpzc) for composite adsorbent. This method involves adding salt to composite adsorbent containing samples and measuring their pH after 48 h following a procedure described elsewhere in (Abewaa et al., 2023a; Fito et al., 2023a). Scanning Electron microscope (SEM), Fourier Transform Infrared Spectroscopy (FTIR), and X-ray Diffraction (XRD)

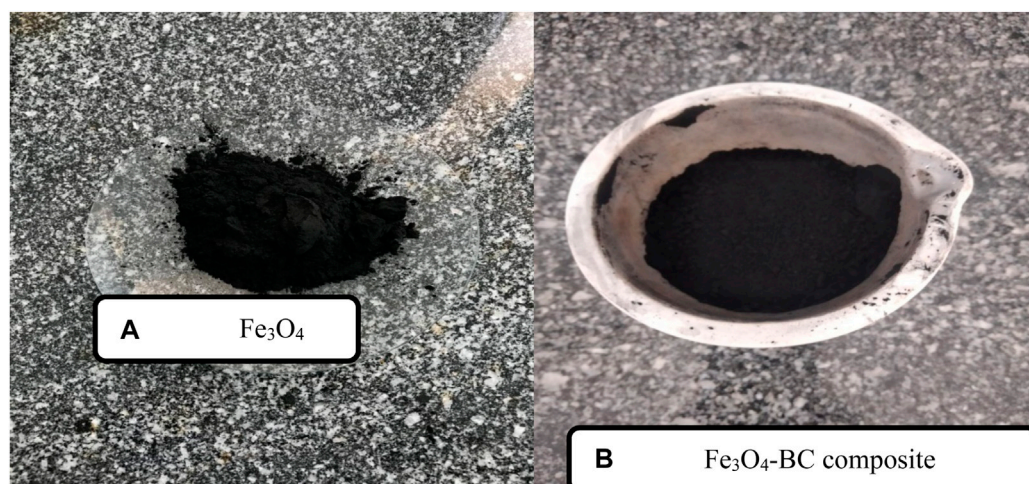


FIGURE 2 Magnetite (A) and Magnetite biochar composite derived from parthenium hysterophorus (B).

TABLE 1 Full factorial experimental design for MB adsorption.

Parameters	Lower	Higher
pH	3	9
Contact time (min)	10	40
MB concentration (mg/L)	100	150
Adsorbent dosage (g/100 mL)	0.01	0.04

characterization procedures are commonly used for the analysis of adsorbent materials. SEM was used to study the morphology and surface structure of adsorbent material (Muttill et al., 2023; Sahu et al., 2023; Veeresh et al., 2023). FTIR was used to identify the functional groups present in the composite adsorbent. XRD analysis was used to determine the crystalline and amorphous nature of the composite adsorbent prepared from magnetite and parthenium hysterophorus biochar. These characterization techniques provide valuable information about the structure, surface properties, and composition of the magnetic biochar, which is important for understanding its adsorption properties and potential applications.

2.3 Batch adsorption experiment

The experimental design employed for the adsorption of MB onto magnetic biochar consisted of four independent variables, each with two levels. The optimization of MB adsorption was achieved through the utilization of a full factorial design. The operating parameters encompassed pH values of 3 and 9, contact times of 20 and 40 min, initial MB concentrations of 100 and 150 mg/L, and adsorbent dosages of 10 and 40 mg per 100 mL, as outlined in Table 1. The batch adsorption process for MB from an aqueous solution was conducted in accordance with previously described procedures. The concentration of methylene blue within the water was determined via UV-Vis spectrophotometry, specifically at a

maximum wavelength of 6,658 nm. A comprehensive calibration curve was established to facilitate this analysis, which is applicable across a broad range of methylene blue concentrations. Finally, the removal efficiency (RE, %) and adsorption capacity (QE, mg/g) are expressed by Eqs 1 and 2 respectively. Here, C_0 (mg/L) and C_f (mg/L) denote the initial and final concentrations of the dye, m represents the mass of the adsorbent in grams, and V signifies the volume of the solution (Obayomi et al., 2023; Wang et al., 2023; Guan et al., 2024).

$$R_E = \frac{C_0 - C_f}{C_0} \times 100\% \quad (1)$$

$$Q_e = (C_0 - C_f) \times \frac{V}{m} \quad (2)$$

2.4 Adsorption isotherm

An adsorption isotherm describes the equilibrium of adsorption of a substance on a solid surface at a constant temperature. It represents the relationship between the amount of adsorbate adsorbed on an adsorbent and the concentration of adsorbate in solution when equilibrium is reached (Mozaffari Majd et al., 2022). Moreover, adsorption isotherms are mathematical equations that quantify the affinity of the adsorbate for the adsorbent (Saleh, 2022). They can accurately describe various adsorption scenarios, including those that consider lateral inter-adsorbate interactions, molecular size, surface heterogeneity, and mobile adsorption (Mozaffari Majd et al., 2022). Additionally, they are used to model experimental equilibrium data and optimize the adsorbent mass in the adsorption process (Dehghani et al., 2021). Adsorption isotherms are essential in understanding the adsorption mechanism and catalytic processes (Russo et al., 2021). Different adsorption models, such as the Freundlich, Langmuir and Temkin isotherms, can be used to fit the experimental data and determine the adsorption capacity and intensity of the adsorbent. In this study, the study of adsorption isotherm was carried out at constant pH (9), contact time (40 min) and adsorbent dosage (0.04 g/100 mL) while varying initial dye

TABLE 2 Isotherm models for the adsorption of MB onto magnetic biochar.

Isotherm model	Linear equation	Parameters
Langmuir	$\frac{1}{Q_e} = \frac{1}{Q_{max}} + \frac{1}{K_L Q_{max}} \times \frac{1}{C_e}$	Q_{max} is a maximum adsorption capacity (mg/g)
		C_e is equilibrium MR concentration mg/L
		K_L is Langmuir isotherm constant (L/mg)
Freundlich	$\log Q_e = \log K_F + \frac{1}{n} \times \log C_e$	K_F - Freundlich constant (mg/g) 1/n-imperial parameter related to intensity of adsorption
Temkin	$Q_e = \frac{RT}{b} \ln C_e + \frac{RT}{b} \ln K_T$	K_T is the equilibrium binding constant (L/mg), b is the Temkin heat of adsorption constant, R is the universal gas constant (8.314 J/Kmol), and T (K) is the system temperature

TABLE 3 Kinetics models for the removal of MB onto magnetite biochar composite.

Kinetic models	Linear equation	Parameters
Pseudo first order (PFO)	$\log(Q_e - Q_t) = \log Q_e - \frac{K_1 \times t}{2.303}$	K_1 -PFO rate constant in (g/(mg min)), t (min)-contact time
		Q_t (mg/g)—adsorption capacity at time t
Pseudo second order (PSO)	$\frac{t}{Q_e} = \frac{1}{K_2 \times Q_e^2} + \frac{t}{Q_e}$	K_2 -PSO rate constant in (g/(mg min))
Intraparticle diffusion (IPD)	$Q_t = K_p \times t^{0.5} + C$	C (mg/L)-intercept
		K_p (mg/(g min ^{0.5}))-IPD rate constant

concentration from 100–150 (100, 110, 120,130, 140 and 150 mg/L). Freundlich, Langmuir and Temkin isotherm models used in this research are shown in Table 2.

2.5 Adsorption kinetics

Adsorption kinetics is the study of the rate at which adsorption occurs. Various mathematical models have been developed to describe this process, including exponential models (Revellame et al., 2020). The kinetics of adsorption can be influenced by factors such as the type of adsorbent and the nature of the adsorbate (Benjelloun et al., 2021). The pseudo first order, pseudo second order and intraparticle diffusion are commonly used to analyze adsorption kinetics, and they can be applied to both local and non-local kinetic equations (Xu et al., 2022). The adsorption process can be divided into two stages: a rapid stage leading to a first phase pseudo-equilibrium, followed by a slower stage leading to a second phase pseudo-equilibrium (Amah and Agunwamba, 2022). Understanding adsorption kinetics is important for various applications, including environmental remediation and the design of adsorption units. In this study, the kinetics investigation of adsorption of MB onto magnetic biochar was carried at a constant adsorbent dosage of 0.04 g/100mL, initial dye concentration of 100 mg/L and pH value of 9 while varying the contact time from 10–40 min (10,15, 20, 25, 30,35 and 40 min). Pseudo first order, pseudo second order and intraparticle diffusion models are presented in Table 3.

2.6 Adsorption thermodynamics

Adsorption thermodynamics involves the study of the thermodynamic properties of adsorption processes, such as

equilibrium constants, Gibbs free energy change (ΔG , kJ/mol) enthalpy change (ΔH , kJ/mol), and entropy change (ΔS , kJ/mol. K). These properties are important for understanding and predicting the mechanism of the adsorption process. Adsorption is a widely used technique in various industries, including water treatment, petroleum refining, gas separation, and air purification. Overall, the study of adsorption thermodynamics in conjunction with adsorption kinetics is essential for a comprehensive understanding of adsorption process. In this research, the investigation of adsorption thermodynamics was done at varying temperatures of 25–45 °C. However, constant values of pH (9), contact time (40 min), initial MB concentration (100 mg/L) and adsorbent dosage of 0.04 g/100 mL were used during thermodynamic investigation. The essential thermodynamic parameters are determined from Eqs 3–6 (Hummadi et al., 2022; Panda et al., 2021; salah omer et al., 2022).

$$\Delta G = -RT \ln k_c \tag{3}$$

$$K_C = \frac{q_e}{C_e} \tag{4}$$

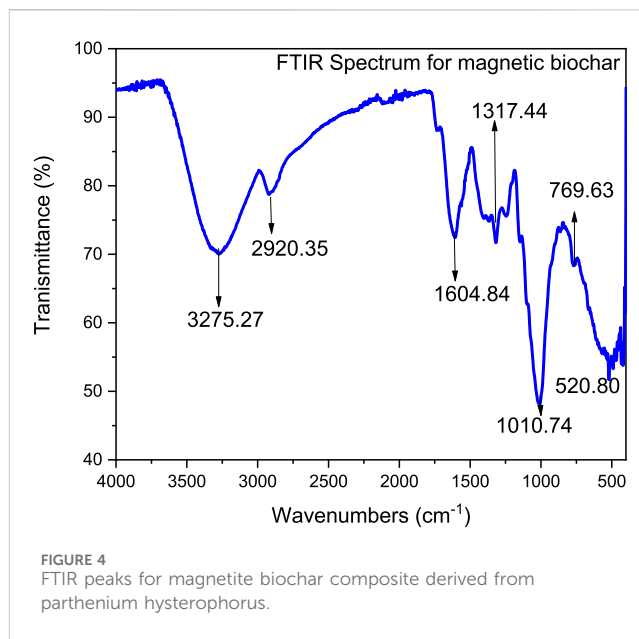
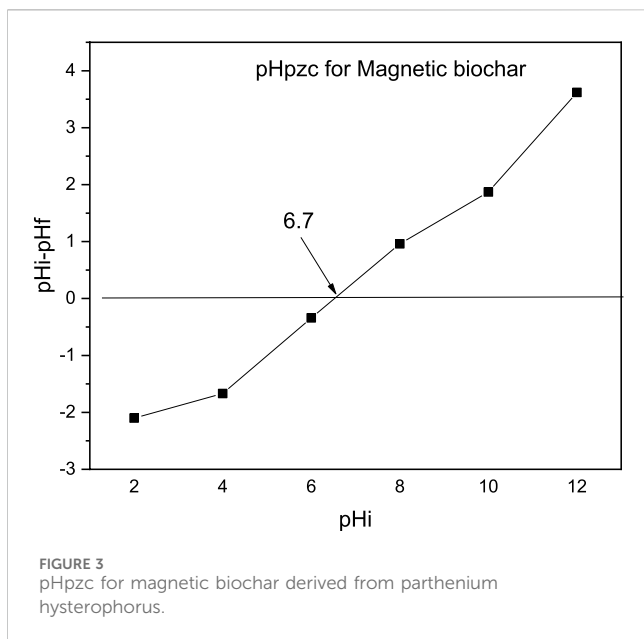
$$\ln k_c = \frac{\Delta S}{R} - \frac{\Delta H}{RT} \tag{5}$$

$$\Delta G = \Delta H - T\Delta S \tag{6}$$

Where K_C is the thermodynamic constant, R is the universal gas constant (8.314 J/mol. K), and T is the absolute temperature in K. From the plot between $\ln k_c$ and $1/T$, the value of ΔH and ΔS was calculated from the slope and intercept obtained.

2.7 Adsorbent regeneration

Composite adsorbents are effective in removing organic dyes and heavy metal ions from water due to their large surface areas

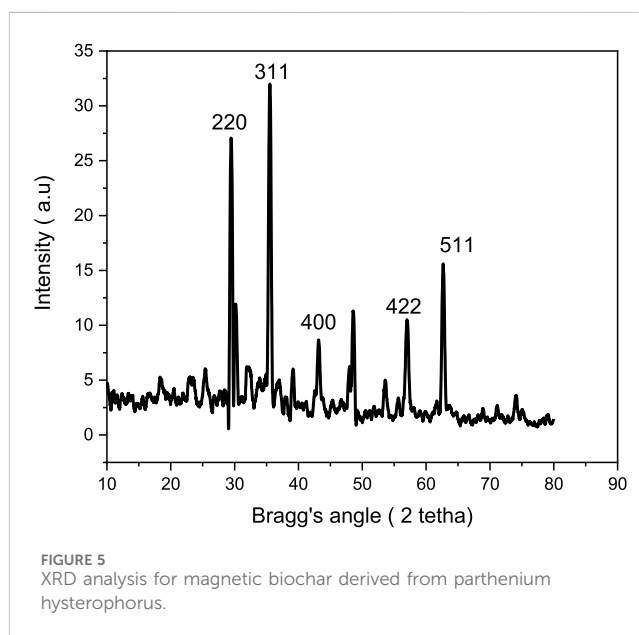


(Futalan et al., 2022). However, pollutants accumulate, leading to a decline in adsorption performance and hazardous solid waste (Jagadeesh and Sundaram, 2023). Recycling waste adsorbents through chemical methods is economically and environmentally effective (Baskar et al., 2022). This study investigates the regenerability and reusability potential of composite adsorbents using a chemical regeneration method using NaOH, which is widely used due to its simplicity and effectiveness. Precisely, pollutant loaded adsorbent was added in to the solution containing 0.1 M NaOH and shaken at 250 rpm for 2 h in order to desorb the pollutant attached to the surface of the composite material. Thereafter, the pollutant desorbed adsorbent material was dried in the oven at 105 °C for 24 h in order to remove the moisture. Finally, MB desorbed magnetic biochar was repeatedly used for five cycles for the adsorption of MB from an aqueous solution following the procedures described in batch adsorption experiments.

3 Results and discussion

3.1 Adsorbent characteristics

The pHpzc of the magnetic biochar derived from parthenium hysterophorus was depicted in Figure 3 and determined to be 6.7. The pHpzc values aid in understanding adsorbent material surface charge, stability, electrolyte interaction, suspension rheology, and ion exchange capacity, and characterize magnetic biochars' adsorption properties at zero charge. Accordingly, the surface of the adsorbent material is positively charged below pH of 6.7 and negative charges dominate the surface of the adsorbent materials above pH of 6.7. This indicated that cationic dyes like MB are sufficiently adsorbed above pH of 6.7 and the reduction in adsorption capacity is expected below pH of 6.7 due to the repulsion between cationic MB dyes and positively charged magnetic surface. A similar finding is reported for magnetite impregnated biochar of parthenium hysterophorus (Fito et al., 2023b).



The functional groups of the composite adsorbent composed of magnetite and parthenium hysterophorus biochar were assessed using FTIR analysis. The number of the functional groups of the adsorbent is presented in Figure 4. This adsorbent showed the presence of many functional groups which indicates the promising adsorbent to interact with many pollutants in the wastewater. The band at 3,275 cm⁻¹ is attributed to O-H stretch vibration, 2,920 cm⁻¹ corresponds to C-H stretch vibration for alkanes, 2,114 cm⁻¹, 1,604 cm⁻¹ corresponds to C=O stretch vibration of carboxylate, 1,317 cm⁻¹ is attributed to C-H bending vibrations (C-H deformation), 1,010 cm⁻¹ corresponds to C-O stretches. The peak at 769 cm⁻¹, is attributed to C-H bending vibration. The peak at 520 cm⁻¹ corresponds to Fe-O indicating successful impregnation of magnetite onto parthenium

hysterophorus-derived biochar (Moges et al., 2022; Abewaa et al., 2023b; Fito et al., 2023b; Fito et al., 2023c; Fito and Ebrahim, 2023).

The X-ray diffraction technique was employed to investigate the crystalline structure of the composite consisting of magnetite and biochar. The findings of the XRD analysis are illustrated in Figure 5. The materials exhibited crystalline properties at specific angles (2θ) of 30.16, 35.53, 43.14, 57.11 and 63.12 corresponding to the peaks (220), (311), (400), (422), and (511), respectively. The predominant peak pattern observed in the composite materials can be attributed primarily to the presence of magnetite in the adsorbent. Given its amorphous nature, the XRD pattern is not expected to reveal the emergence of peaks related to parthenium hysterophorus-derived biochar. These outcomes align closely with the findings reported by Fito et al. (2023), where magnetic biochar material exhibited peaks at angles of 30.15, 35.51, 43.16, 53.32, and 57.08 (Fito et al., 2023b).

The examination of the surface morphology of the biochar-magnetite composite obtained from a sample of parthenium hysterophorus was conducted using Scanning Electron microscope (SEM). The SEM analysis produced an image, as presented in Figure 6. Within this study, the surface of the composite material was magnified by a factor of 300, enabling the observation of distinct pore sizes and their distributions. It was observed that the composite adsorbent possessed highly irregular surfaces characterized by a significant level of heterogeneity, as well as the presence of cavities, holes, ruptures, voids, fractures, fissures, nooks, and crannies. These attributes play a critical role in enhancing the sorption capacity of the surface. Additionally, the high temperatures experienced during the carbonization and calcination processes result in the release of volatile matter from the microstructure of the particles. This phenomenon leads to the creation of voids on the surfaces of the adsorbent, ultimately transforming into pores. Generally, the heterogeneous surfaces of the adsorbent provide an advantageous setting for the adsorption of various pollutants from water and wastewater (Albatmi et al., 2022).

3.2 Batch adsorption performance

The full factorial design comprising four parameters at two levels was utilized in this research giving a total experimental runs of 32 in duplicate. The maximum removal efficiency attained in this study was reduced the initial dye concentration from 100 to 0.001 giving a maximum removal efficiency of 99.99%. This maximum removal efficiency was recorded at optimum treatment conditions of pH 9, contact time of 40 min, initial dye concentration of 100 mg/L and adsorbent dosage of 0.04 g/100 mL. On the other hand, the minimum removal efficiency recorded was determined to be 49.34%. The huge gap between the maximum and minimum removal efficacies indicates the significance of the effects of the operating parameters (Waghmare et al., 2023). Table 4 presents the adsorption capability of magnetic biochar derived from parthenium hysterophorus applied in the decontamination of MB from an aqueous solution. The maximum removal efficiency (99.99%) of MB attained utilizing magnetite doped biochar of parthenium hysterophorus is higher than the maximum removal efficiency (94%) attained using activated carbon derived from the same material (Fito et al., 2020). Magnetite doping enhances the adsorption capacity of Rumex abyssinicus derived biochar compared to plain biochar due to several factors. Firstly, the

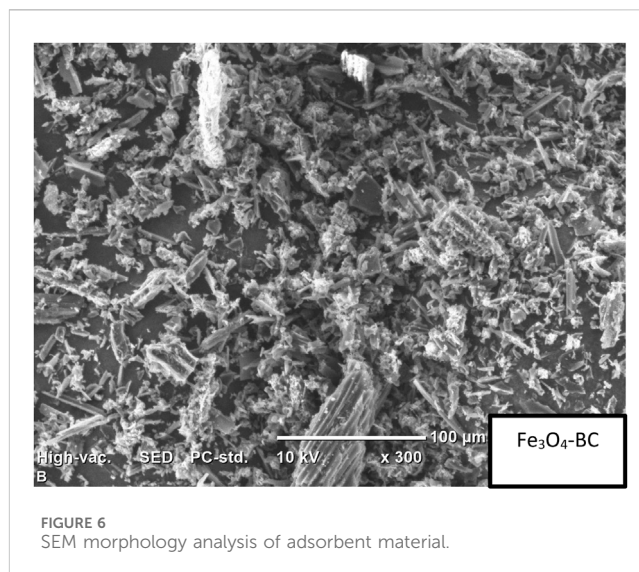


FIGURE 6
SEM morphology analysis of adsorbent material.

deposition of iron minerals on the carbon surface creates additional sorption sites, increasing the sorption ability of the biochar. Secondly, the presence of magnetite in the biochar composite leads to the activation of effective aggregates, resulting in improved adsorption performance for MB molecules (Xie et al., 2021; Guo et al., 2023).

The maximum adsorption capacity recorded in this study is compared with various magnetic biochars applied for the removal of MB from wastewater and aqueous solution. As a result, the recent study is found to be superior compared to many previous researches, providing a promising solution for the detoxification of MB saturated effluents. Table 5 presents a comprehensive comparative analysis of various biomass based magnetic biochars applied for the removal of MB.

3.3 Effect of operating parameters on MB removal efficiency

3.3.1 Effect of adsorbent dosage

The effect of adsorbent dosage on the adsorption performances of MB onto magnetic biochar was conducted by varying the adsorbent dosage from 0.01–0.04 g/100 mL while keeping all the other parameters at optimum values as shown in Figure 7. Fundamentally, the effect of adsorbent dosage is paramount since it determines the adsorption capacity of the adsorbent. In this study, the MB concentration (100 mg/L), contact time (40 min) and pH of 9 were used constantly to investigate the influence of adsorbent dosage variation on MB dye adsorption performance. As a result, it was observed that increasing the adsorbent dosage increased the removal efficiency. Precisely, as adsorbent dosage increased from 0.01–0.04 g/100 mL, the removal efficiency increased from 85.6% to 99.98%. Conversely, the adsorption capacity decreased from 856 mg/g to 249.95 mg/g as an adsorbent dosage increased from 0.01 to 0.04 g/100 mL (Figure 8) attributed to the inverse relationship between adsorption capacity and adsorbent dosage for fixed initial dye concentration and volume of the solution. The increase of adsorption performance (percentage removal

TABLE 4 Batch adsorption performance of MB removal onto magnetic biochar.

Run	pH	MB concentration (mg/L)	Adsorbent dosage (g/100 mL)	Contact time (min)	Removal efficiency (%)
1.	9	100	0.01	40	75.69
2.	9	150	0.01	10	49.34
3.	3	100	0.01	40	75.14
4.	3	150	0.04	10	70.62
5.	9	100	0.04	40	99.99
6.	3	100	0.01	10	66.09
7.	9	150	0.01	40	64.56
8.	9	100	0.04	10	93.2
9.	9	150	0.04	10	71.17
10.	3	150	0.01	40	65.10
11.	3	100	0.04	10	91.75
12.	3	150	0.04	40	77.86
13.	9	100	0.01	10	64.14
14.	9	150	0.04	40	80.48
15.	3	100	0.04	40	95.23
16.	3	150	0.01	10	51.89

TABLE 5 Comparative study of different magnetic biochars applied for the removal of MB.

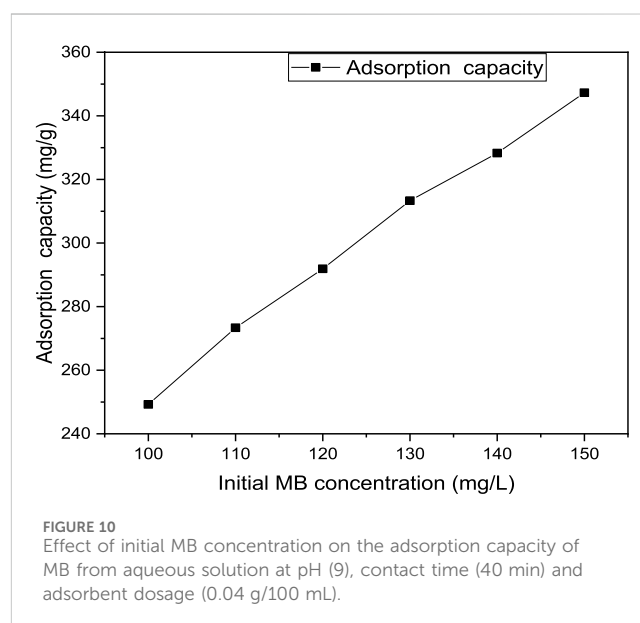
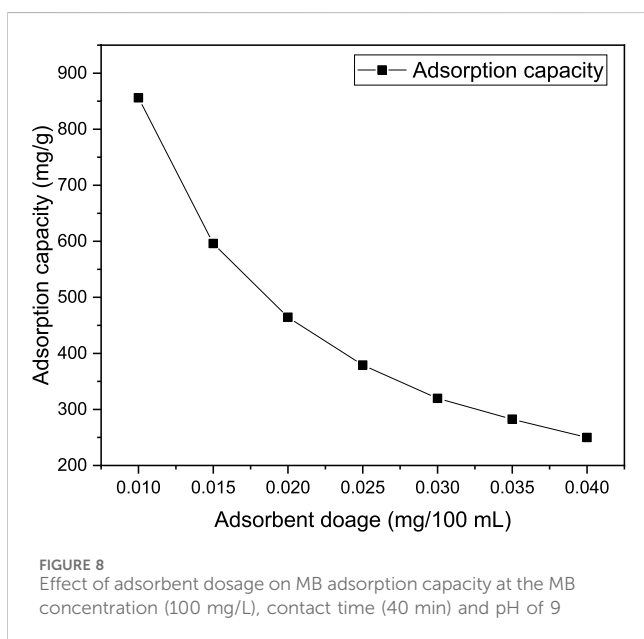
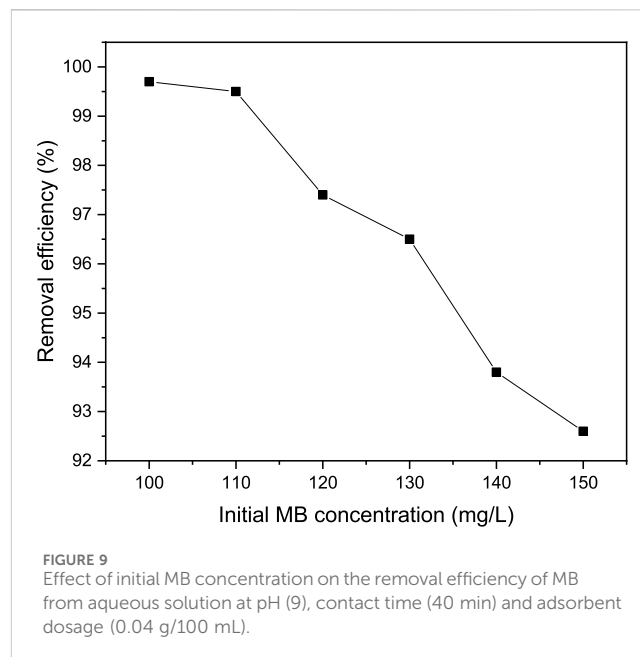
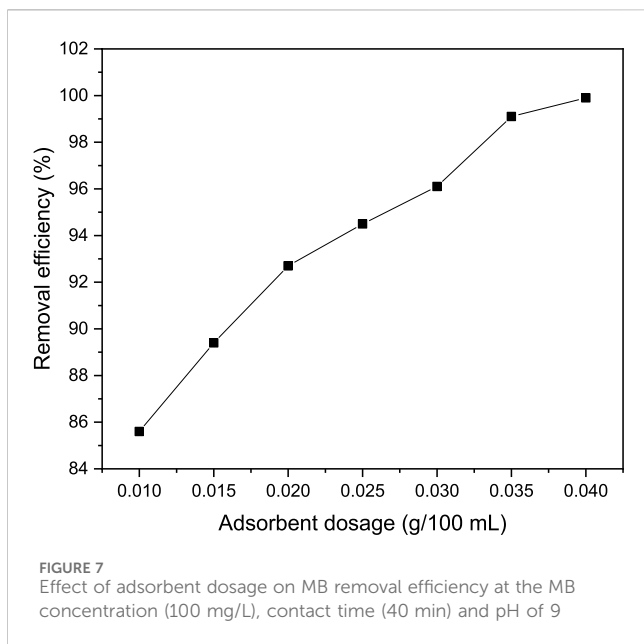
S.No	Adsorbent	Adsorption capacity (mg/g)	References
1.	Corn stalks biochar-Fe ₃ O ₄	84.6	Yan et al. (2023)
2.	waste sludge biochar- Fe ₃ O ₄	5.92	Manoko et al. (2022)
3.	Fe ₃ O ₄ - pea biochar	175.44	Rubangakene et al. (2023)
4.	Ulva fasciata marine algae biochar- Fe ₃ O ₄	50.12	Kumar et al. (2024)
5.	magnetic tea residue biochar	82.81	Mu et al. (2022)
6.	Wakame biochar- Fe ₃ O ₄	117.58	Yao et al. (2020)
7.	corn stalk biochar- Fe ₃ O ₄	153.5	Yan et al. (2023)
8.	Parthenium hysterophorus biochar- Fe ₃ O ₄	327.87	This research

efficiency) with increasing adsorbent dosage is attributed to the presence of sufficient active sites as the adsorbent gets increased in dosage. Moreover, a higher dosage of adsorbent provides more surface area for adsorption, allowing for more dye molecules to be adsorbed. The increase in adsorbent dosage leads to a higher concentration of adsorbent particles in the solution, increasing the chances of contact between the dye molecules and the adsorbent surface, resulting in higher removal efficiency (Dimbo et al., 2024). Similar trend was observed in khat stem based activated carbon applied for the removal of MB from textile wastewater (Takele et al., 2023).

3.3.2 Effect of initial MB dye concentration

MB removal efficiency and adsorption capacity are significantly influenced by initial MB concentration. Normally, the relationship

between available active sites and the concentration of the dye molecules is crucial in increasing or decreasing the decolorization of the target pollutant. During the effect of the initial MB concentration investigation, the concentration of MB was varied from 100–150 mg/L while all other factors such as pH, contact time and adsorbent dosage were fixed at their optimum values of 9, 40 min and 0.04 g/100 mL respectively. As can be observed from Figure 9, as the initial MB concentration increases from 100–150 mg/L, the removal efficiency decreases from 99.7% to 92.6%. However, Figure 10 shows the increasing trend of adsorption capacity from 249.25 to 347.25 mg/g with increasing initial MB concentration. Moreover, the maximum removal efficiency of MB was achieved at a minimum initial concentration of dye (100 mg/L). Afterwards, the removal percentage gradually decreased as the initial dye concentration

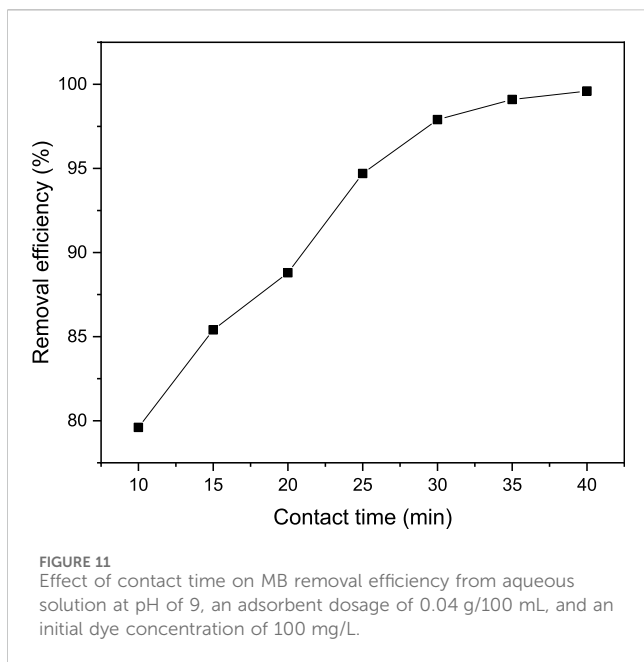


was raised. This might be because the adsorption sites were fixed and reached saturation. Hence, with an increase in initial dye concentration, no further adsorption could be achieved so that percentage removal experiences a decrease. A similar trend has been also investigated by (El-sayed et al., 2014) who worked on the assessment of activated carbon prepared from corncob by chemical activation with phosphoric acid. In general, higher initial concentrations of MB result in a higher number of dye molecules in the solution, leading to a higher competition for active sites on the adsorbent material. As a result, the available active sites become saturated more quickly, reducing the overall removal efficiency (Dinh et al., 2021; Nowicki et al., 2022; Mahmoudi et al., 2023). Additionally, the increased concentration of MB can lead to a higher

mass transfer resistance, making it more difficult for the adsorbent to effectively remove the dye molecules from the solution (Bharathi and Ramesh, 2013).

3.3.3 Effect of contact time

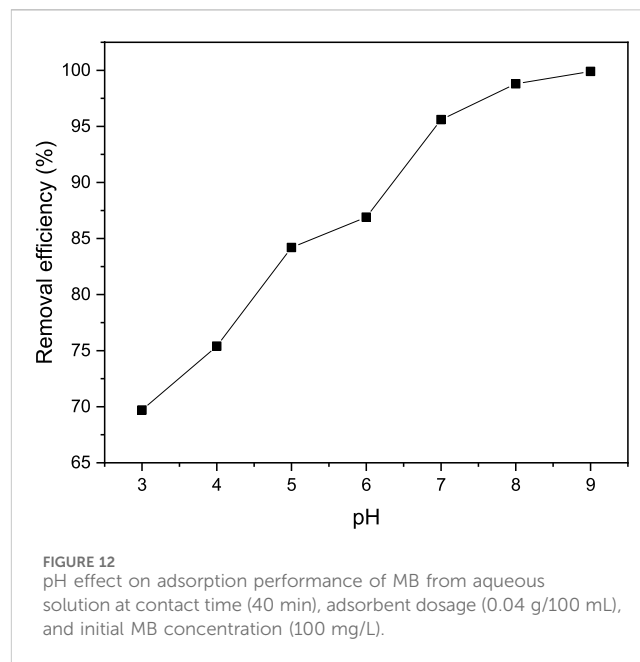
The duration for which the pollutant and adsorbent come into contact with each other holds significant importance in the treatment of wastewater using adsorption techniques. This is primarily due to the fact that the contact time affects the rate at which the dye is absorbed and provides insight into the step that controls the rate of adsorption of the targeted pollutant. Furthermore, in adsorption processes, the contact time



determines the mechanism involved in the migration of the dye from the bulk of the solution to the surface of the adsorbent, as well as the diffusion of the dye through the boundary layer and into the interior pores of the adsorbent. In this particular study, the impact of the contact time on the adsorption performance of MB from an aqueous solution was examined by varying the contact time from 10 to 40 min, while maintaining all other operating parameters (pH, adsorbent dosage, and initial MB concentration) constant. Figure 11 illustrates the effects of contact time on the efficiency of MB removal at a fixed pH of 9, an adsorbent dosage of 0.04 g/100 mL, and an initial dye concentration of 100 mg/L. Consequently, an increase in MB removal efficiency from 79.6% to 99.6% was observed as the contact time increased from 10 to 40 min. This rise in the efficiency of removing the targeted pollutant with longer contact time can be attributed to the availability of sufficient time for the interaction between the adsorbate and the adsorbent. Additionally, in the adsorption process, a longer contact time allows for more opportunities for the methylene blue molecules to come into contact with the adsorbent material, increasing the chances of adsorption and removal (Hakim and Supartono, 2021; Al-abbasi et al., 2022; Mohammadi and Jafari, 2023; Ni et al., 2023).

3.3.4 Effect of PH

A range of pH values ranging from 3 to 9 was utilized to examine the impact of pH on the efficacy of MB removal from a solution. Conversely, fixed values of contact time (40 min), adsorbent dosage (0.04 g/100 mL), and initial MB concentration (100 mg/L) were employed to investigate the influence of pH on the efficiency of MB removal. The findings of the investigation into the effect of pH on MB removal efficiency are illustrated in Figure 12. The figure reveals that the percentage of removal increases as the pH value rises. This phenomenon can be attributed to the fact that the surface of the adsorbent material is typically negatively charged above the pH_{pzc}, resulting in a lower percentage of MB removal in the lower pH range.



Additionally, the acidic environment causes an increase in the concentration of hydrogen ions, which subsequently neutralizes the negatively charged carbon surface, thereby reducing the adsorption of the positively charged dye cation due to a decrease in the attractive force between the adsorbent and adsorbate. The pH of a solution can affect the point of zero charge (pH_{pzc}) of a magnetite-doped biochar composite, which in turn influences its adsorption capacity for methylene blue. The pH_{pzc} is the pH at which the surface of the biochar has a neutral charge, meaning the adsorption of H⁺ and OH⁻ ions is equal. However, it is known that the pH_{pzc} of biochars can influence the adsorption process under certain pH conditions. When the pH of the solution is above pH_{pzc}, negative charges dominate the surface of the composite materials enhancing the attraction of positively charged MB dye and the magnetite doped biochar of parthenium hysterophorus. However, at pH of the solution less than pH_{pzc}, there is repulsion between the positive charges on the adsorbent material and the positively charged MB dye, thereby decreasing the adsorption capacity. Hence, the maximum removal efficiency obtained pH 9 supports the pH_{pzc} concept as the pH_{pzc} of magnetite biochar composite is determined to be 6.7.

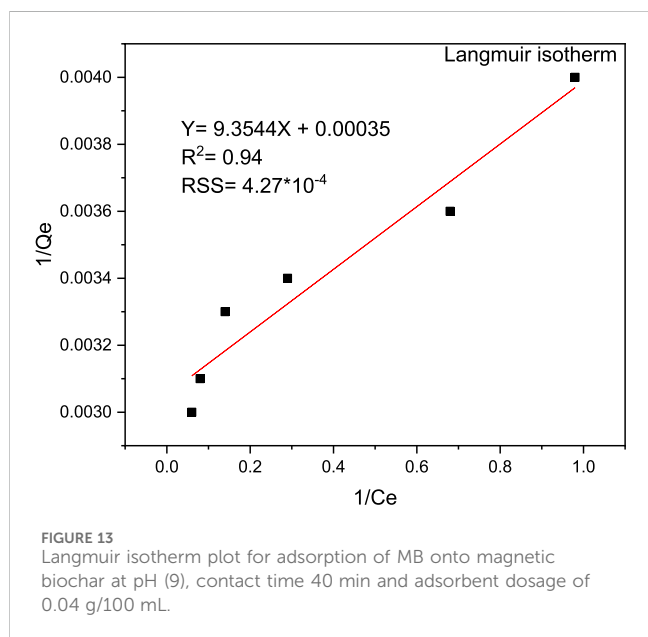
In line with this, the surface negative charges of adsorbent material increase with an increase in pH, enhancing its adsorption ability towards positively charged MB (Info, 2021). As depicted in the graph, a pH value of 9 can be considered the optimal pH. It was observed that a maximum removal efficiency of 99.92% was achieved at a pH of 9.

3.4 Interaction effects of operating parameters on the MB removal efficiency

In addition to individual effects on the adsorption performance of MB from onto magnetic biochar, it is crucial

TABLE 6 ANOVA for interactive regression model.

Source	Sum of squares	df	Mean square	F-value	p-value	
Model	3310.67	10	331.07	3102.31	<0.0001	significant
A-pH	1.49	1	1.49	14.00	0.0134	
B-MB concentration	1059.67	1	1059.67	9929.75	<0.0001	
C-Adsorbent dosage	1771.36	1	1771.36	16598.76	<0.0001	
D-Contact time	359.58	1	359.58	3369.46	<0.0001	
AB	1.40	1	1.40	13.10	0.0152	
AC	12.02	1	12.02	112.67	0.0001	
AD	6.11	1	6.11	57.29	0.0006	
BC	55.76	1	55.76	522.54	<0.0001	
BD	12.44	1	12.44	116.60	0.0001	
CD	30.83	1	30.83	288.90	<0.0001	
Residual	0.5336	5	0.1067			
Cor Total	3311.20	15				



to consider the interaction effects among the operating parameters. In this regard, the batch adsorption performance data (Table 4) was fed to the design expert software version 11 and the interaction among different operating parameters was statistically analyzed. Accordingly, the batch adsorption performance data accurately fit to interactive regression model with adjusted and projected R² values of 0.9995 and 0.9983 respectively. Additionally, all the interaction between the operating factors is found significant (as their p-value is determined to be less than 0.05), which highlights the significant effect on the MB removal efficiency. Herein, the interaction of pH and initial MB concentration is found to have a negative effect on the removal efficiency of MB. Individually, the pH is

determined to have an encouraging effect on the MB removal efficiency. Conversely, the individual effect of initial MB concentration at fixed values of contact time, adsorbent dosage and pH was determined to have a negative effect on the adsorption performance of MB dye. The interaction effect of pH and adsorbent dosage as well as pH and contact time is determined to positively affect the removal efficiency of the MB dye. On the other hand, the MB removal efficiency is negatively affected by the interaction of initial MB concentration and adsorbent dosage as well as adsorbent dosage and contact time. However, the interaction of initial MB concentration and contact time is found to have a positive impact on the MB removal efficiency. Table 6 presents the interactive model describing the adsorption pattern of MB adsorption onto magnetite biochar composite derived from parthenium hysterophorus. The relative impact of significant factors as their interaction on MB removal efficiency is presented in Eq. 6, whereas Eq. 7 presents the model equation for the removal of MB onto magnetic biochar.

$$C > B > D > BC > CD > BD > AC > AD > A > AB \quad (7)$$

$$\text{Removal efficiency} = 74.52 + 0.3056 A - 8.14 B + 10.52 C + 4.74 D - 0.2956 AB + 0.8669 AC + 0.6181 AD - 1.87 BC + 0.8819 BD - 1.39 CD \quad (9)$$

3.5 Adsorption isotherm

The Langmuir, Freundlich, and Temkin isotherms were visually depicted in Figures 13, 14, 15, respectively. The determination coefficients (R²) for the Langmuir, Freundlich, and Temkin isotherms were found to be 0.94, 0.98, and 0.97, respectively. Additionally, residual sum of squares (RSS) used for error analysis of data fit to each isotherm models is provided. The Freundlich isotherm provided the best fit for the data, indicating

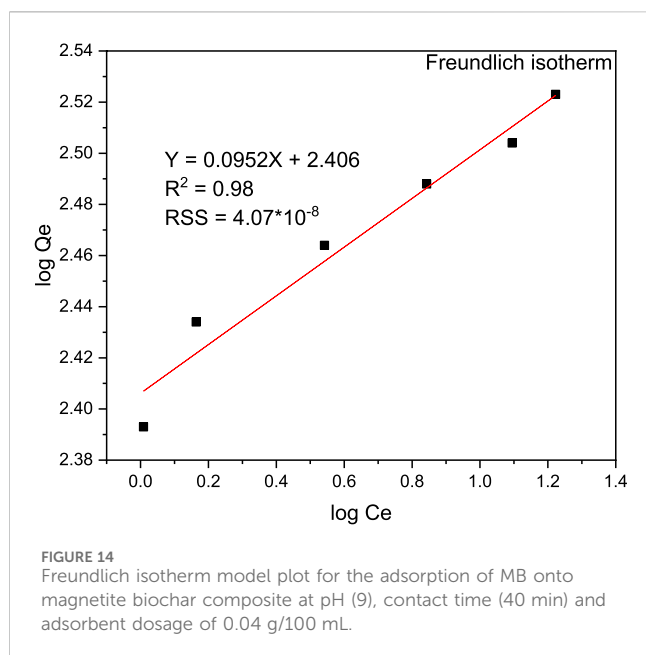


FIGURE 14
Freundlich isotherm model plot for the adsorption of MB onto magnetite biochar composite at pH (9), contact time (40 min) and adsorbent dosage of 0.04 g/100 mL.

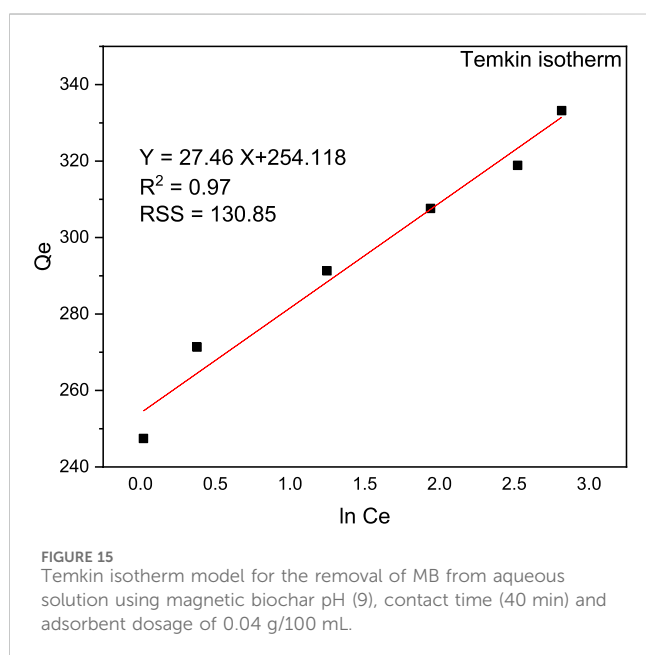


FIGURE 15
Temkin isotherm model for the removal of MB from aqueous solution using magnetic biochar pH (9), contact time (40 min) and adsorbent dosage of 0.04 g/100 mL.

a multilayer and heterogeneous adsorption process. Consequently, the surface of the adsorbent was determined to be heterogeneous, and the adsorption of MB occurred on the active sites of the multilayer surface. Moreover, the Langmuir isotherm exhibited a Q_{\max} value of 327.87 mg/g and a K_L value of 0.0003 g/L, showcasing the effectiveness of the adsorption process. On the other hand, the Langmuir isotherm feasibility (R_L) and the Freundlich isotherm constant related to intensity ($1/n$) were determined to be 0.99 and 0.095, respectively, indicating a favorable adsorption process. The recorded value of $1/n$ in this study was 0.397, which is low, suggesting higher heterogeneity. In a favorable Freundlich isotherm (i.e., $n > 1$), active sites with the highest binding

energies are utilized first for less heterogeneous surfaces, followed by weaker sites for more heterogeneous surfaces. The present study yielded a higher Freundlich adsorption capacity (K_F) of 254.68 (mg/g)/(mg/L)^{0.095}. Furthermore, a higher K_F value indicates a lower free energy requirement for the adsorption process. The Temkin isotherm constants K_T and B_T were determined to be 16.693 L/g and 90.27 J/mol, respectively. Overall, the isotherm study showed that the adsorption of MB onto magnetic biochar is favourable with multilayer and heterogeneous surface interactions.

3.6 Adsorption kinetics

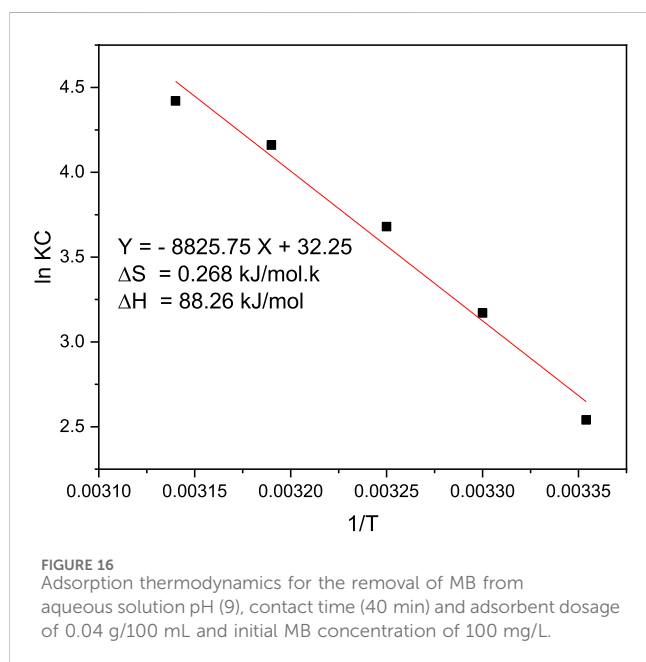
The kinetics of dye adsorption was investigated using the optimum conditions determined from the batch experiments. Table 7 presents the calculated adsorption capacities (Q_e , cal), experimental adsorption capacities (Q_e , exp), and values of parameters such as K_1 , K_2 and K_p for all three kinetic models. The pseudo second order reaction adsorption kinetics exhibited a coefficient of determination (R^2) of 0.99, while the pseudo first order reaction kinetics showed a lower value of R^2 (0.91). Therefore, given the higher coefficient of determination and the negligible difference between the equilibrium and calculated adsorption capacities (Q_e , exp) and (Q_e , calc), it can be concluded that the pseudo second order model provides a better description of the cationic dye adsorption kinetics. Moreover, the rate-limiting adsorption mechanism was found to be chemisorption, which occurs due to the formation of chemical bonds between the adsorbate molecules and specific surface locations (active sites) on the magnetic biochar. Additionally, an intraparticle diffusion model was developed to examine the adsorbate's ability to penetrate the interior surface of the adsorbent. The intraparticle diffusion rate constant (K_p) and the C (mg/g) values were determined to be 1.25 mg/(g.min^{0.5}) and 64.27 mg/g respectively. These findings indicate that the adsorption rate is influenced by both the adsorbate and the adsorbent and that intraparticle diffusion does not solely control the adsorption process.

3.7 Adsorption thermodynamics

The adsorption thermodynamics of MB adsorption onto magnetic biochar derived from parthenium hysterophorus was investigated employing the Van't Hof equation and the result of the analyses is presented in Figure 16. The thermodynamic parameters provide insights into the spontaneity, endothermicity, and feasibility of the adsorption process for methylene blue onto the magnetite-doped biochar composite. The values of ΔG indicate the feasibility of the process, with negative values indicating a spontaneous adsorption process. The values of ΔH indicate the endothermic nature of the process, with positive values indicating that heat is absorbed during adsorption. The values of ΔS indicate the increase in disorder during the adsorption process, with positive values indicating an increase in randomness. From the thermodynamics study, it can be observed that the value of ΔG was determined to have negative values throughout the study. Moreover, the values for both ΔH and ΔS were determined to be positive. Overall, the combination of negative ΔG , positive ΔH , and

TABLE 7 Kinetics parameters for the adsorption of MB onto magnetite biochar composite derived from parthenium hysterophorus.

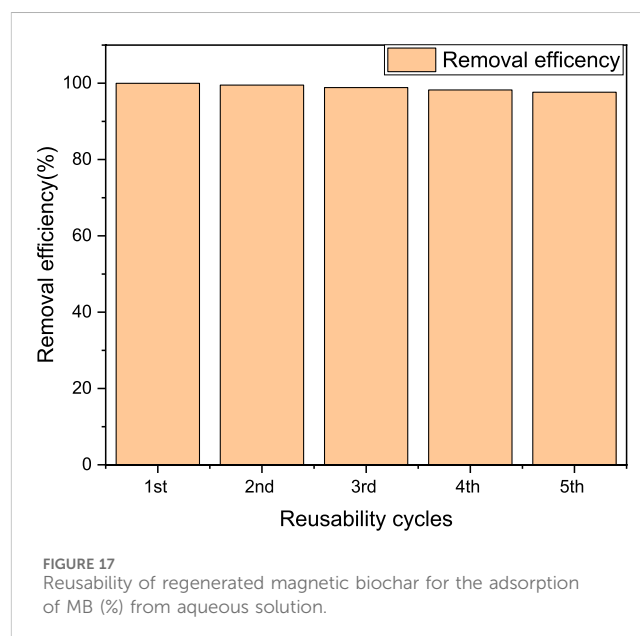
Kinetic model	Kinetic parameters	Parameter values
Pseudo first order	Q_e exp (mg/g)	331.25
	Q_e calc (mg/g)	275.43
	K_1 (g/(mg. min))	0.258
	R^2	0.91
Pseudo second order	Q_e exp (mg/g)	331.25
	Q_e calc (mg/g)	330.98
	K_2 (g/(mg. min))	2.674
	R^2	0.99
Intraparticle diffusion model	K_p (mg/(g. min ^{0.5}))	1.25
	C (mg/g)	64.27
	R^2	0.96



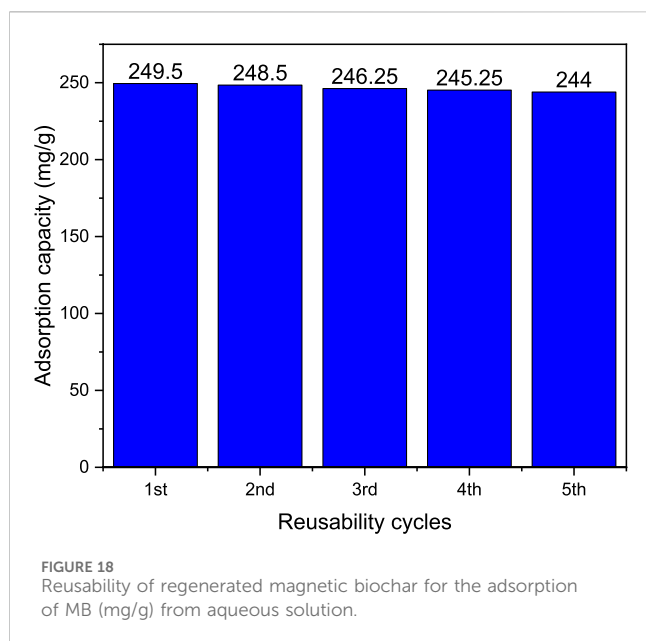
positive ΔS suggests that the adsorption process is spontaneous, endothermic, and feasible for the removal of MB onto the magnetite-doped biochar of parthenium hysterophorus.

3.8 Reusability of the adsorbent

The assessment of reusability over multiple cycles provides insight into the practical applicability and sustainability of magnetite biochar derived from Parthenium hysterophorus as an adsorbent for industrial-scale decolorization of methylene blue wastewater effluent. The ability of the magnetite biochar to maintain its adsorption capacity and efficiency over multiple cycles demonstrates its potential for practical use in wastewater treatment. The reusability of the magnetite biochar is attributed to



its stability and the presence of magnetic nanoparticles, which allow for easy separation and regeneration of the adsorbent. The biochar-magnetite composite derived from parthenium hysterophorus was tested for MB removal for five times, evaluating the adsorption efficiency during adsorption-desorption cycles. In the initial stage, the adsorption efficiency was recorded as 99.8%, but decreased to 97.6% by the fifth cycle as shown in Figure 17. This decline indicates a slight reduction in adsorption performances as the number of cycles increased. The loss of active sites associated with incomplete desorption likely contributed to this decrease in performance. The reusability performance of magnetic biochar derived from parthenium hysterophorus is further presented in adsorption capacity as shown in Figure 18. As can be observed from Figure 18, the adsorption capacity for five consecutive cycles of reusability ranged from 249.5 to 244 mg/g. Additionally, the insignificant decrease in removal capacity after each cycle,



demonstrates the adsorbent's ability to be regenerated and reused. These findings confirm that the biochar-magnetite composite is highly reusable and stable, making it a promising candidate for practical applications in MB removal.

4 Conclusion

In this study, a magnetic composite adsorbent derived from biochar of parthenium hysterophorus and magnetite was prepared through pyrolysis and coprecipitation techniques. The adsorbent has characteristics like heterogeneous and porous morphology, crystalline structure, and numerous functional groups, making it effective in removing pollutants from water and wastewater. On the other hand, the maximum and minimum removal efficiencies recorded in this study were determined to be 99.99% and 49.34% respectively. The effects of operating parameters such as pH, contact time, initial MB concentration and adsorbent dosage were thoroughly investigated. Accordingly, the removal efficiency of MB was discovered to increase with increasing pH, contact time and adsorbent dosage. However, initial MB concentration and removal efficiency were found to have a negative relationship. The isotherm and kinetics studies were investigated and the Freundlich isotherm model ($R^2 = 0.98$) and pseudo second order ($R^2 = 0.99$) gave the best fitting with experimental data suggesting multilayer interaction and chemisorption nature respectively. Finally, the magnetite biochar composite is highly regenerated and reusable which highlights its effectiveness in removing MB saturated effluent at an industrial scale.

References

Abewaa, M., Adino, E., and Mengistu, A. (2023a). Preparation of Rumex abyssinicus based biosorbent for the removal of methyl orange from aqueous solution. *Heliyon* 9 (12), e22447. doi:10.1016/j.heliyon.2023.e22447

Data availability statement

The original contributions presented in the study are included in the article/supplementary material, further inquiries can be directed to the corresponding author.

Author contributions

MT: Conceptualization, Investigation, Methodology, Validation, Visualization, Writing–original draft, Writing–review and editing. MG: Writing–review and editing, Data curation, Methodology, Format analysis. MD: Writing–review editing, Supervision, Validation, Visualization

Funding

The author(s) declare that no financial support was received for the research, authorship, and/or publication of this article.

Acknowledgments

We want to express my sincere gratitude to the University of Johannesburg for its dedication to creating a lively and supportive research environment, as their support has given us an invaluable opportunity to delve deeply into the research. We have succeeded in my research endeavors because of the state-of-the-art facilities, access to cutting-edge resources, and collaborative atmosphere. In addition, we would like to express our gratitude to Adama and Addis Ababa Science and Technology Universities for their support of our laboratory facilities.

Conflict of interest

The author declares that the research was conducted in the absence of any commercial or financial relationships that could be construed as a potential conflict of interest.

Publisher's note

All claims expressed in this article are solely those of the authors and do not necessarily represent those of their affiliated organizations, or those of the publisher, the editors and the reviewers. Any product that may be evaluated in this article, or claim that may be made by its manufacturer, is not guaranteed or endorsed by the publisher.

Abewaa, M., Mengistu, A., Takele, T., Fito, J., and Nkambule, T. (2023b). Adsorptive removal of malachite green dye from aqueous solution using Rumex abyssinicus derived activated carbon. *Sci. Rep.* 13 (1), 14701. doi:10.1038/s41598-023-41957-x

- Ahmed, J., Thakur, A., and Goyal, A. (2021). *Industrial wastewater and its toxic effects*. London, United Kingdom: Royal Society of Chemistry.
- Ahuja, R., Kalia, A., Sikka, R., and Chaitra, P. (2022). Nano modifications of biochar to enhance heavy metal adsorption from wastewaters: a review. *ACS Omega* 7 (50), 45825–45836. doi:10.1021/acsomega.2c05117
- Ajiboye, T. O., Oyewo, O. A., and Onwudiwe, D. C. (2021). Simultaneous removal of organics and heavy metals from industrial wastewater: a review. *Chemosphere* 262, 128379. doi:10.1016/j.chemosphere.2020.128379
- Al-abbasi, A., Alammaw, M., and Abdulljoad, S. (2022). Removal of methyl orange dye from aqueous solutions using amberlite LA-2 as an extractant. *J. Pure Appl. Sci.* 21 (2), 55–60. doi:10.51984/jopas.v21i2.2055
- Al-Asadi, S. T., Al-Qaim, F. F., Al-Saedi, H. F. S., Deyab, I. F., Kamyab, H., and Chelliapan, S. (2023). Adsorption of methylene blue dye from aqueous solution using low-cost adsorbent: kinetic, isotherm adsorption, and thermodynamic studies. *Environ. Monit. Assess.* 195 (6), 676. doi:10.1007/s10661-023-11334-2
- Albatrni, H., Qiblawey, H., and Al-Marri, M. J. (2022). Walnut shell based adsorbents: a review study on preparation, mechanism, and application. *J. Water Process Eng.* 45, 102527. doi:10.1016/j.jwpe.2021.102527
- Alouiz, I., Benhadj, M., Elmoutassir, D., Mouadili, A., Sennoune, M., Amarouch, M.-Y., et al. (2023). Optimization of methylene blue dye removal adsorbed on olive pomace derived activated charcoal: isotherm, kinetic and thermodynamic studies.
- Amah, V. E., and Agunwamba, J. C. (2022). Exponential model for adsorption kinetics. *J. Eng. Res. Rep.*, 35–41. doi:10.9734/jerr/2022/v23i8741
- Anae, J., Ahmad, N., Kumar, V., Thakur, V. K., Gutierrez, T., Yang, X. J., et al. (2021). Recent advances in biochar engineering for soil contaminated with complex chemical mixtures: remediation strategies and future perspectives. *Sci. Total Environ.* 767, 144351. doi:10.1016/j.scitotenv.2020.144351
- Astuti, W., Meysanti, D., Salsabila, M. T., Sulistyarningsih, T., and Rusiyanto, (2023). Photodegradation of methylene blue dye by hematite-biochar composite prepared from *Dendrocalamus asper* using microwave-assisted pyrolysis (MAP). *IOP Conf. Ser. Earth Environ. Sci.* 1203 (1), 012053. doi:10.1088/1755-1315/1203/1/012053
- Azanaw, A., Birlie, B., Teshome, B., and Jemberie, M. (2022). Textile effluent treatment methods and eco-friendly resolution of textile wastewater. *Case Stud. Chem. Environ. Eng.* 6, 100230. doi:10.1016/j.csee.2022.100230
- Babuji, P., Thirumalaisamy, S., Duraisamy, K., and Periyasamy, G. (2023). Human health risks due to exposure to water pollution: a review. *Water* 15 (14), 2532. doi:10.3390/w15142532
- Baskar, A. V., Bolan, N., Hoang, S. A., Sooriyakumar, P., Kumar, M., Singh, L., et al. (2022). Recovery, regeneration and sustainable management of spent adsorbents from wastewater treatment streams: a review. *Sci. Total Environ.* 822, 153555. doi:10.1016/j.scitotenv.2022.153555
- Batool, M., Khan, W. ud D., Hamid, Y., Farooq, M. A., Naeem, M. A., and Nadeem, F. (2022). Interaction of pristine and mineral engineered biochar with microbial community in attenuating the heavy metals toxicity: a review. *Appl. Soil Ecol.* 17, 104444. doi:10.1016/j.apsoil.2022.104444
- Bedada, D., Angassa, K., Tiruneh, A., Kloos, H., and Fito, J. (2020). Chromium removal from tannery wastewater through activated carbon produced from *Parthenium hysterophorus* weed. *Environ. Ecol. Environ. Sci.* 5 (3), 184–195. doi:10.1007/s40974-020-00160-8
- Benjelloun, M., Miyah, Y., Akdemir Evrendilek, G., Zerrouq, F., and Lairini, S. (2021). Recent advances in adsorption kinetic models: their application to dye types. *Arabian J. Chem.* 14 (4), 103031. doi:10.1016/j.arabj.2021.103031
- Bharathi, K. S., and Ramesh, S. T. (2013). Removal of dyes using agricultural waste as low-cost adsorbents: a review. *Appl. Water Sci.* 3 (4), 773–790. doi:10.1007/s13201-013-0117-y
- Bužga, M., Machytka, E., Dvořáčková, E., Švagera, Z., Stejskal, D., Máca, J., et al. (2022). Methylene blue: a controversial diagnostic acid and medication? *Toxicol. Res.* 11 (5), 711–717. doi:10.1093/toxres/tafac050
- Chhimwal, M., Pandey, D., and Srivastava, R. K. (2022). “Pristine biochar and engineered biochar: differences and application,” in *Engineered biochar: fundamentals, preparation, characterization and applications* (Springer), 3–19.
- Dehghani, M. H., Gholami, S., Karri, R. R., Lima, E. C., Mahvi, A. H., Nazmara, S., et al. (2021). Process modeling, characterization, optimization, and mechanisms of fluoride adsorption using magnetic agro-based adsorbent. *J. Environ. Manag.* 286, 112173. doi:10.1016/j.jenvman.2021.112173
- Dhruv Patel, D., and Bhatt, S. (2022). Environmental pollution, toxicity profile, and physico-chemical and biotechnological approaches for treatment of textile wastewater. *Biotechnol. Genet. Eng. Rev.* 38 (1), 33–86. doi:10.1080/02648725.2022.2048434
- Dimbo, D., Abewaa, M., Adino, E., Mengistu, A., Takele, T., Oro, A., et al. (2024). Methylene blue adsorption from aqueous solution using activated carbon of *spathodea campanulata*. *Results Eng.* 21, 101910. doi:10.1016/j.rineng.2024.101910
- Dinh, N. T., Vo, L. N. H., Tran, N. T. T., Phan, T. D., and Nguyen, D. B. (2021). Enhancing the removal efficiency of methylene blue in water by fly ash via modified adsorbent with alkaline thermal hydrolysis treatment. *RSC Adv.* 11 (33), 20292–20302. doi:10.1039/d1ra02637b
- Ejaz, U., Khan, S. M., Aqeel, M., Khalid, N., Sarfraz, W., Naeem, N., et al. (2022). Use of *Parthenium hysterophorus* with synthetic chelator for enhanced uptake of cadmium and lead from contaminated soils—a step toward better public health. *Front. Public Health* 10, 1009479. doi:10.3389/fpubh.2022.1009479
- El-sayed, G. O., Yehia, M. M., and Asaad, A. A. (2014). Assessment of activated carbon prepared from corncob by chemical activation with phosphoric acid. *Water Resour. Industry* 7–8, 66–75. doi:10.1016/j.wri.2014.10.001
- Feng, Z., Yuan, R., Wang, F., Chen, Z., Zhou, B., and Chen, H. (2021). Preparation of magnetic biochar and its application in catalytic degradation of organic pollutants: a review. *Sci. Total Environ.* 765, 142673. doi:10.1016/j.scitotenv.2020.142673
- Fito, J., Abewaa, M., Mengistu, A., Angassa, K., Ambaye, A. D., Moyo, W., et al. (2023a). Adsorption of methylene blue from textile industrial wastewater using activated carbon developed from *Rumex abyssinicus* plant. *Sci. Rep.* 13 (1), 5427. doi:10.1038/s41598-023-32341-w
- Fito, J., Abewaa, M., and Nkambule, T. (2023b). Magnetite - impregnated biochar of parthenium hysterophorus for adsorption of Cr (VI) from tannery industrial wastewater. *Appl. Water Sci.* 13 (3), 78–23. doi:10.1007/s13201-023-01880-y
- Fito, J., Abrham, S., and Angassa, K. (2020). Adsorption of methylene blue from textile industrial wastewater onto activated carbon of parthenium hysterophorus. *Int. J. Environ. Res.* 14 (5), 501–511. doi:10.1007/s41742-020-00273-2
- Fito, J., Ebrahim, O., and Nkambule, T. T. I. (2023). The application Mn - Ni ferrite nanocomposite for adsorption of chromium from textile industrial wastewater. *Water, Air, & Soil Pollut.* 234, 37. doi:10.1007/s11270-022-06058-x
- Fito, J., Mengistu, A., Abewaa, M., Angassa, K., Moyo, W., Phiri, Z., et al. (2023c). Adsorption of Black MNN reactive dye from tannery wastewater using activated carbon of *Rumex Abyssinicus*. *J. Taiwan Inst. Chem. Eng.* 151, 105138. doi:10.1016/j.jtice.2023.105138
- Frolova, L. (2019). *Synthesis of magnetic biochar for efficient removal of Cr (III)*.
- Futalan, C. M., Choi, A. E. S., Soriano, H. G. O., Cabacungan, M. K. B., and Millare, J. C. (2022). Modification strategies of kapok fiber composites and its application in the adsorption of heavy metal ions and dyes from aqueous solutions: a systematic review. *Int. J. Environ. Res. Public Health* 19 (5), 2703. doi:10.3390/ijerph19052703
- Gautam, D. R. (2019). Water pollution: its ethical aspects and management. *Int. J. Res. Appl. Sci. Eng. Technol.* 7 (2), 486–493. doi:10.22214/ijraset.2019.2067
- Ghazali, M. N., Sinniah, U. R., and Ahmad-Hamdani, M. S. (2023). Parthenium hysterophorus weed fecundity and seed survival at different soil pH and burial conditions. *Pertanika J. Trop. Agric. Sci.* 46 (2), 593–606. doi:10.47836/pjtas.46.2.13
- Guan, F., Tao, J., Yao, Q., Li, Z., Zhang, Y., Feng, S., et al. (2024). Alginate-based aerogel fibers with a sheath-core structure for highly efficient methylene blue adsorption via directed freezing wet-spinning. *Colloids Surfaces A Physicochem. Eng. Aspects* 680, 132706. doi:10.1016/j.colsurfa.2023.132706
- Guo, D., Wu, J., Feng, D., Zhang, Y., Zhu, X., Luo, Z., et al. (2023). Mechanism of efficient magnetic biochar for typical aqueous organic contaminant combined-adsorption removal. *Fuel Process. Technol.* 247, 107795. doi:10.1016/j.fuproc.2023.107795
- Hakim, H. M. A., and Supartono, W. (2021). Removal of methylene blue from water using sugar palm agro industry waste adsorbent. *IOP Conf. Ser. Earth Environ. Sci.* 667 (1), 012008. doi:10.1088/1755-1315/667/1/012008
- Hummedi, K. K., Luo, S., and He, S. (2022). Adsorption of methylene blue dye from the aqueous solution via bio-adsorption in the inverse fluidized-bed adsorption column using the torrefied rice husk. *Chemosphere* 287 (P1), 131907. doi:10.1016/j.chemosphere.2021.131907
- Info, A. (2021). Removal of methylene blue from water by polyacrylonitrile-Cosodium methallylsulfonate copolymer (AN69) and polysulfone (PSf) synthetic membranes. *Prog. Color, Colorants Coatings* 14, 89–100. doi:10.30509/pccc.2021.81690
- Islam, T., Li, Y., and Cheng, H. (2021). Biochars and engineered biochars for water and soil remediation: a review. *Sustain. Switz.* 13 (17), 9932–10025. doi:10.3390/su13179932
- Jagadeesh, N., and Sundaram, B. (2023). Adsorption of pollutants from wastewater by biochar: a review. *J. Hazard. Mater. Adv.* 9, 100226. doi:10.1016/j.hazadv.2022.100226
- Jones, E. R., Bierkens, M. F. P., van Puijenbroek, P. J. T. M., van Beek, L., Rens, P. H., Wanders, N., et al. (2023). Sub-Saharan Africa will increasingly become the dominant hotspot of surface water pollution. *Nat. Water* 1 (7), 602–613. doi:10.1038/s44221-023-00105-5
- Kazemi Shariat Panahi, H., Dehghani, M., Ok, Y. S., Nizami, A. S., Khoshnevisan, B., Mussato, S. I., et al. (2020). A comprehensive review of engineered biochar: production, characteristics, and environmental applications. *J. Clean. Prod.* 270, 122462. doi:10.1016/j.jclepro.2020.122462
- Khan, W. U., Ahmed, S., Dhoble, Y., and Madhav, S. (2023). A critical review of hazardous waste generation from textile industries and associated ecological impacts. *J. Indian Chem. Soc.* 100 (1), 100829. doi:10.1016/j.jics.2022.100829
- Kishor, R., Purchase, D., Saratale, G. D., Saratale, R. G., Ferreira, L. F. R., Bilal, M., et al. (2021). Ecotoxicological and health concerns of persistent coloring pollutants of textile industry wastewater and treatment approaches for environmental safety. *J. Environ. Chem. Eng.* 9 (2), 105012. doi:10.1016/j.jece.2020.105012
- Kumar, K., Gnida, A., Turek-szytow, J., Saad, M., Gregor, M., Matula, G., et al. (2024). Chemical Engineering Research and Design Design of innovative hybrid biochar

- prepared from marine algae and magnetite, *Insights into Adsorpt. Perform. Mech.* 201, 218–227. doi:10.1016/j.cherd.2023.11.053
- Lebrun, M., Miard, F., Renouard, S., Nandillon, R., Scippa, G. S., Morabito, D., et al. (2018). Effect of Fe-functionalized biochar on toxicity of a technosol contaminated by Pb and As: sorption and phytotoxicity tests. *Environ. Sci. Pollut. Res.* 25, 33678–33690. doi:10.1007/s11356-018-3247-9
- Li, H., Kong, J., Zhang, H., Gao, J., Fang, Y., Shi, J., et al. (2023). Mechanisms and adsorption capacities of ball milled biomass fly ash/biochar composites for the adsorption of methylene blue dye from aqueous solution. *J. Water Process Eng.* 53, 103713. doi:10.1016/j.jwpe.2023.103713
- Mahmoudi, S., Otadi, M., Hekmati, M., Monajjemi, M., and Shekarabi, A. S. (2023). Methylene blue removal from aqueous solution using modified Met-SWCNT-Ag nanoparticles: optimization using RSM-CCD. *Int. J. Chem. React. Eng.* 21 (10), 1177–1197. doi:10.1515/ijcre-2022-0240
- Malik, S., Singh, S., Pooja, M. R., Padhan, S. R., and Radheshyam, (2023). Growth behavior of parthenium hysterophorus as influenced by environmental factors. *Int. J. Environ. Clim. Change* 13 (8), 1158–1168. doi:10.9734/ijec/2023/v13i82055
- Manoko, M. C., Chirwa, E. M. M., and Makgopa, K. (2022). Non-demineralized paper waste sludge derived magnetic biochar as sorbs for removal of methylene blue, phosphorus, and selenate in wastewater. *Clean. Chem. Eng.* 3, 100048. doi:10.1016/j.cce.2022.100048
- Meena, M., Yadav, G., Sonigra, P., and Shah, M. P. (2022). A comprehensive review on application of bioreactor for industrial wastewater treatment. *Lett. Appl. Microbiol.* 74 (2), 131–158. doi:10.1111/lam.13557
- Mishra, D., Jain, S., Khare, P., and Singh, R. (2023). Comparative investigation of biochar-based nanocomposites over pristine biochar: an overview. *Biochar-Based Nanocomposites Contam. Manag.*, 57–68. doi:10.1007/978-3-031-28873-9_5
- Moges, A., Nkambule, T. T. I., and Fito, J. (2022). The application of GO-Fe 3 O 4 nanocomposite for chromium adsorption from tannery industry wastewater. *J. Environ. Manag.* 305, 114369. doi:10.1016/j.jenvman.2021.114369
- Mohammadi, A. A., and Jafari, A. (2023). Degradation of methylene blue in aqueous phase by homogenous and heterogeneous catalytic Ozonation.
- Mozaffari Majd, M., Kordzadeh-Kermani, V., Ghalandari, V., Askari, A., and Sillanpää, M. (2022). Adsorption isotherm models: a comprehensive and systematic review (2010–2020). *Sci. Total Environ.* 812, 151334. doi:10.1016/j.scitotenv.2021.151334
- Mu, Y., Du, H., He, W., and Ma, H. (2022). Functionalized mesoporous magnetic biochar for methylene blue removal: performance assessment and mechanism exploration. *Diam. Relat. Mater.* 121, 108795. doi:10.1016/j.diamond.2021.108795
- Muche, M., Molla, E., Mohammed, S., Sintie, E., and Hassen, A. (2022). Evaluating slow pyrolysis of parthenium hysterophorus biochar: perspectives to acidic soil amelioration and growth of selected wheat (*Triticum aestivum*) varieties. *Sci. World J.* 2022, 1–13. doi:10.1155/2022/8181742
- Murtaza, G., Ahmed, Z., Dai, D., Iqbal, R., Bawazeer, S., Usman, M., et al. (2022). A review of mechanism and adsorption capacities of biochar-based engineered composites for removing aquatic pollutants from contaminated water. *Front. Environ. Sci.* 10. doi:10.3389/fenvs.2022.1035865
- Mustapha, O. R., Osobamiro, T. M., Sanyaolu, N. O., and Alabi, O. M. (2023). Adsorption study of Methylene blue dye: an effluents from local textile industry using Pennisetum pupureum (elephant grass). *Int. J. Phytoremediation* 25, 1348–1358. doi:10.1080/15226514.2022.2158781
- Muttill, N., Jagadeesan, S., Chanda, A., Duke, M., and Kumar Singh, S. (2023). Characterisation of activated carbon derived from carbon black produced by the pyrolysis of waste tyres. *Adv. Mater. Process. Technol.*, 1–11. doi:10.1080/2374068x.2023.2192327
- Ni, Z., Lu, H., Han, Y., and Zha, X. (2023). Degradation of methylene blue aqueous solution using atmospheric pressure dielectric barrier discharge. *Anal. Chem. A J* 2 (1), 17–24. doi:10.23977/anal.2023.020103
- Nowicki, P., Gruszczynska, K., Urban, T., and Wiśniewska, M. (2022). Activated biocarbons obtained from post-fermentation residue as potential adsorbents of organic pollutants from the liquid phase. *Physicochem. Problems Mineral Process.* 58 (2), 1–12. doi:10.37190/ppmp/146357
- Obayomi, K. S., Lau, S. Y., Zahir, A., Meunier, L., Jianhua, Z., Dada, A. O., et al. (2023). Removing methylene blue from water: a study of sorption effectiveness onto nanoparticles-doped activated carbon. *Chemosphere* 313, 137533. doi:10.1016/j.chemosphere.2022.137533
- Oladoye, P. O., Ajiboye, T. O., Omotola, E. O., and Oyewola, O. J. (2022). Methylene blue dye: toxicity and potential technologies for elimination from (waste) water. *Results Eng.* 100678. doi:10.1016/j.rineng.2022.100678
- Panda, S. K., Aggarwal, I., Kumar, H., Prasad, L., Kumar, A., Sharma, A., et al. (2021). Magnetite nanoparticles as sorbents for dye removal: a review. *Environ. Chem. Lett.* 19 (3), 2487–2525. doi:10.1007/s10311-020-01173-9
- Pereira, C. P., Goldenstein, J. P. N., and Bassin, J. P. (2022). Industrial wastewater contaminants and their hazardous impacts. *Biosorption Wastewater Contam.*, 1–22. doi:10.1002/9781119737629.ch1
- Posso, M. C., Domingues, F. C., Ferreira, S., and Silvestre, S. (2022). Development of phenothiazine hybrids with potential medicinal interest: a review. *Molecules* 27 (1), 276. doi:10.3390/molecules27010276
- Rajendran, S., Priya, A. K., Kumar, P. S., Hoang, T. K. A., Sekar, K., Chong, K. Y., et al. (2022). A critical and recent developments on adsorption technique for removal of heavy metals from wastewater-A review. *Chemosphere* 303, 135146. doi:10.1016/j.chemosphere.2022.135146
- Revellame, E. D., Fortela, D. L., Sharp, W., Hernandez, R., and Zappi, M. E. (2020). Adsorption kinetic modeling using pseudo-first order and pseudo-second order rate laws: a review. *Clean. Eng. Technol.* 1, 100032. doi:10.1016/j.clet.2020.100032
- Rubangakene, N. O., Elkady, M., Elwardany, A., Fujii, M., Sekiguchi, H., and Shokry, H. (2023). Effective decontamination of methylene blue from aqueous solutions using novel nano-magnetic biochar from green pea peels. *Environ. Res.* 220, 115272. doi:10.1016/j.envres.2023.115272
- Russo, A. V., Merlo, B. G., and Jacobo, S. E. (2021). Adsorption and catalytic degradation of Tartrazine in aqueous medium by a Fe-modified zeolite. *Clean. Eng. Technol.* 4, 100211. doi:10.1016/j.clet.2021.100211
- Sahu, A., Sen, S., and Mishra, S. C. (2023). A comparative study on characterizations of biomass derived activated carbons prepared by both normal and inert atmospheric heating conditions. *J. Indian Chem. Soc.* 100 (4), 100943. doi:10.1016/j.jics.2023.100943
- salah omer, A., A.El Naeem, G., Abd-Elhamid, A. I., Farahat, O., O. M., El-Bardan, A. A., Soliman, H., M. A., et al. (2022). Adsorption of crystal violet and methylene blue dyes using a cellulose-based adsorbent from sugarcane bagasse: characterization, kinetic and isotherm studies. *J. Mater. Res. Technol.* 19, 3241–3254. doi:10.1016/j.jmrt.2022.06.045
- Saleh, T. A. (2022). Isotherm models of adsorption processes on adsorbents and nanoadsorbents. *Interface Sci. Technol.* 34, 99–126. doi:10.1016/B978-0-12-849876-7.00009-9
- Santoso, E., Ediaty, R., Kusumawati, Y., Bahruji, H., Sulistiono, D. O., and Prasetyoko, D. (2020). Review on recent advances of carbon based adsorbent for methylene blue removal from waste water. *Mater. Today Chem.* 16, 100233. doi:10.1016/j.mtchem.2019.100233
- Schweitzer, L., and Noblet, J. (2018). Water contamination and pollution. *Green Chem.*, 261–290. doi:10.1016/b978-0-12-809270-5.00011-x
- Sutar, S., and Jadhav, J. (2024). A comparative assessment of the methylene blue dye adsorption capacity of natural biochar versus chemically altered activated carbons. *Bioresour. Technol. Rep.* 25, 101726. doi:10.1016/j.biteb.2023.101726
- Takele, T., Angassa, K., Abewaa, M., Kebede, A. M., and Tessema, I. (2023). Adsorption of methylene blue from textile industrial wastewater using activated carbon developed from H3PO4-activated khat stem waste. *Biomass Convers. Biorefinery*, 1–24. doi:10.1007/s13399-023-05245-y
- Tang, W., Pei, Y., Zheng, H., Zhao, Y., Shu, L., and Zhang, H. (2022). Twenty years of China's water pollution control: experiences and challenges. *Chemosphere* 295, 133875. doi:10.1016/j.chemosphere.2022.133875
- Veeresh, S., Ganesha, H., Nagaraj, Y. S., and Devendrappa, H. (2023). Structural, morphological characterization of nitric acid and Potassium hydroxide activated carbon composite. *Mater. Today Proc.* doi:10.1016/j.matpr.2023.06.156
- Waghmare, C., Ghodmare, S., Ansari, K., Dehghani, M. H., Khan, M. A., Hasan, M. A., et al. (2023). Experimental investigation of H3PO4 activated papaya peels for methylene blue dye removal from aqueous solution: evaluation on optimization, kinetics, isotherm, thermodynamics, and reusability studies. *J. Environ. Manag.* 345, 118815. doi:10.1016/j.jenvman.2023.118815
- Wang, H., Yang, L., Qin, Y., Chen, Z., Wang, T., Sun, W., et al. (2023). Highly effective removal of methylene blue from wastewater by modified hydroxyl groups materials: adsorption performance and mechanisms. *Colloids Surfaces A Physicochem. Eng. Aspects* 656 (PA), 130290. doi:10.1016/j.colsurfa.2022.130290
- Wen, Z., Xi, J., Lu, J., Zhang, Y., Cheng, G., Zhang, Y., et al. (2021). Porous biochar-supported MnFe2O4 magnetic nanocomposite as an excellent adsorbent for simultaneous and effective removal of organic/inorganic arsenic from water. *J. Hazard. Mater.* 411, 124909. doi:10.1016/j.jhazmat.2020.124909
- Xie, J., Lin, R., Liang, Z., Zhao, Z., Yang, C., and Cui, F. (2021). Effect of cations on the enhanced adsorption of cationic dye in Fe3O4-loaded biochar and mechanism. *J. Environ. Chem. Eng.* 9 (4), 105744. doi:10.1016/j.jece.2021.105744
- Xu, S., Jin, Y., Li, R., Shan, M., and Zhang, Y. (2022). Amidoxime modified polymers of intrinsic microporosity/alginate composite hydrogel beads for efficient adsorption of cationic dyes from aqueous solution. *J. Colloid Interface Sci.* 607, 890–899. doi:10.1016/j.jcis.2021.08.157
- Yan, N., Hu, B., Zheng, Z., Lu, H., Chen, J., Zhang, X., et al. (2023). Twice-milled magnetic biochar: a recyclable material for efficient removal of methylene blue from wastewater. *Bioresour. Technol.* 372, 128663. doi:10.1016/j.biortech.2023.128663
- Yao, X., Ji, L., Guo, J., Ge, S., Lu, W., Cai, L., et al. (2020). Magnetic activated biochar nanocomposites derived from wakame and its application in methylene blue adsorption. *Bioresour. Technol.* 302, 122842. doi:10.1016/j.biortech.2020.122842
- Zahoor, I., and Mushtaq, A. (2023). Water pollution from agricultural activities: a critical global review. *Int. J. Chem. Biochem. Sci.* 23, 164–176.